RSC Advances

ROYAL SOCIETY OF CHEMISTRY

www.rsc.org/advances

Journal Name

ARTICLE

Low Temperature Processed ITO Free Perovskite Solar Cells Without Hole Transport Layer

Received 00th January 20xx,
Accepted 00th January 20xx

DOI: 10.1039/x0xx00000x

www.rsc.org/

Tang Liu , Lijian Zuo, Tao Ye, Jiake Wu, Guobiao Xue, Weifei Fu, Hongzheng Chen*

Perovskite solar cells (PSCs) have been considered as a promising photovoltaic technology due to their attractive power conversion efficiency (PCE) exceeding 20% and easy of their processability at low temperature. However, there were a few reports on low temperature processed ITO-free PSCs. In this work, highly transparent and conductive poly(3,4-ethylenedioxythiophene):polystyrene sulfonate (HC-PEDOT:PSS, PH1000) was employed as electrode as an alternative material of ITO. PSCs built on three different electrodes (PH1000-5%, PH1000-10% and PH1000-H) with or without hole transport layer (HTL) were fabricated. The factors that influence the performance of PSCs such as conductivity, morphology, work function and wettability of the electrode, morphology of perovskite films and different electrode treatments were investigated. A comparison of different electrodes as well as their corresponding impact on the device performance were also presented. The optimized average PCE of 7.95% with the highest PCE up to 9.65% for PSCs built on PH1000-10% electrode without HTL was achieved. When a layer of PEDOT:PSS was spin coated on PH1000-H to prevent perovskite from decomposing, the optimized PCE of 6.98% with the highest up to 9.31% was achieved. Our results indicate that PH-1000 is a promising material to replace both ITO electrode and HTL, providing a much simpler architecture for flexible PSC applications.

1. Introduction

PSCs have been considered as a promising photovoltaic technology due to their superb power conversion efficiency (PCE) exceeding 20%[1]. In addition to their high efficiency, PSCs have also shown great promise in low cost manufacture[2-6]. However, most of the PSCs are built on transparent conductive oxides[7,8] (TCOs) electrode, which is an expensive component in PSCs. The most common TCOs to date are tin doped indium oxide[9,10] (ITO) and fluorine-doped tin oxide[11] (FTO), which have several drawbacks such as high energy cost of processing and inherent brittleness. Indium diffusion into the active layers is also one of the problem when ITO contacts with PEDOT:PSS because ITO has a relatively high solubility in acidic solution[12]. Also these materials are not abundant in nature. Therefore, it's necessary to develop low cost transparent electrode materials to replace TCOs for highly efficient PSCs[13,14].

Many transparent electrode materials[8, 15-19] can be viable substitute for TCOs that have already been widely applied in organic solar cells (OSCs). But not all these transparent electrodes are suitable for PSCs and few reports concern this issue[20, 21]. In addition, there are only some reports on the application of transparent electrode in PSCs[22]. Cao *et al*[20] first demonstrated PSCs using silver nanowires as the front electrode in PSCs. Silver nanowires[23, 24] have advantages of low sheet resistance (15-25 Ω sq^{-1}), high transparency (80-90%) and mechanical flexibility. However, silver can react with halogen in perovskite, leading to a quick break down of conductive network. To solve this problem, a thick layer of ZnO and TiO_2 was deposited as a barrier layer, which however resulted in poor charge transport property and performance. Jun *et al*[25] deposited an ultra-thin silver membrane on PSCs that fabricated on Ti substrate (the structure of solar cells is Ti substrate/dense TiO_2 layer /mesoporousTiO_2/$CH_3NH_3PbI_3$/ 2,2',7,7'-tetrakis-(N,N-di-p-methoxy-phenylamine)-9,9'bi-fluorene(spiro-OMeTAD)/Ultra- thin metal film. The PSCs showed a PCE of about 6% which was limited by the transmittance of silver membrane. Watson *et al*[26] reported flexible PSCs built on Ti substrate with a PCE up to 10.3% by using Ni nanomesh embedded PET as transparent electrode. However, most of the TCO-free solar cells reported now consist a layer of compact TiO_2 which needs high temperature processing[20, 26, 27, 28]. These studies suggest that metal nanowire electrodes are not suitable in this type of PSCs.

Recently, Kelly *et al*[21] reported PSCs with average PCEs of 4±2% built on highly conductive poly(3,4-ethylenedioxythiophene):polystyrene sulfonate (HC-PEDOT:PSS). HC-PEDOT:PSS exhibits many advantages, such as low cost, compatible with roll-to-roll[29, 30] processing, and low sheet resistance. Dianetti *et al*[13] also reported PSCs built on HC-PEDOT:PSS with a PCE of 4.9%. But the factors to achieve high efficiency was not studied in details. On the other hand, hole transport layer

*address: State Key Laboratory of Silicon Materials, MOE Key Laboratory of Macromolecular Synthesis and Functionalization, Department of Polymer Science & Engineering, Zhejiang University, Hangzhou 310027, P. R. China
*E-mail: hzchen@zju.edu.cn

(HTL) also bears a large portion of production cost of the PCSs which is undesirable for further commercialization. Though there are some reports on HTL-free PSCs showing impressive PCE exceeding 10%[31, 32], few of them are based on TCO-free PCSs.

In this work, we demonstrated TCO-free PSCs with a PCE up to 9.65% based on high conductive HC-PEDOT:PSS[33, 34] transparent electrode fabricated at low temperature (lower than 140°C) in an inverted device geometry. Because HC-PEDOT:PSS has the function to transport hole charge carriers, our designed TCO-free PSCs feature high performance with no HTL which simplified the process of PSCs. Our results indicate that HC-PEDOT:PSS is a promising material to replace both ITO and HTL, providing a much simpler architecture for flexible PSC applications.

2. Experimental

2.1. Materials and methods

HC-PEDOT:PSS (Clevios PH1000) and PEDOT:PSS (Clevios P VP.AI4083) were purchased from Haraeus Corporation. HC-PEDOT:PSS was used to prepare the transparent electrode instead of ITO while PEDOT:PSS was used as the hole transport material, which are denoted as PH1000 and PEDOT:PSS, respectively. $PbCl_2$, CH_3NH_3I, (6,6)-phenyl-C61-butyric acid methyl ester ($PC_{61}BM$), and the OTHER MATERIALS WERE BOUGHT FROM SIGMA-ALDRICH.

ZnO nanoparticles (NPs) were synthesized by a sol-gel process using zinc acetate and tetramethylammonium hydroxide (TMAH) reported by elsewhere[35].

The atomic forcemicroscope (AFM) images were obtained using a Veeco Multimode AFM (VeecoIIIa) with the tapping mode. UV-vis absorption spectra and transmittance spectra were taken on a Shimadzu UV-2450 spectrometer. The SEM images and energy dispersive X-ray spectroscopy (EDX) were taken on a S-4800 (Hitachi) field-emission scanning electron microscope (FESEM).

The current density–voltage (*J–V*) curves of PSCs were measured with a Keithley 2400 measurement source units. The photocurrent was measured under a calibrated solar simulator (Abet 300 W) at 100 mW cm^{-2}, and the light intensity was calibrated with a standard silicon photovoltaic reference cell. External quantum efficiency (EQE) spectra were measured witha Stanford lock-in amplifier 8300 unit. Water contact angle was measured by an Optical contact angle measuring instrument (KRUSS DSA100). Ultraviolet photoelectron spectroscopy (UPS) was conducted on an ESCALAB Ultra X-ray photoelectron spectroscopy (VA ESCALAB MARK II) equipped with a monochromatized Al Kα X-ray source.

2.2. Solar cell fabrication

Glass was cleaned sequentially by deionized water, detergent, acetone, isopropanol and ethanol ultrasonic bath for 20 min followed by ultraviolet UV-Ozone treatment for 20 min.

2.2.1. ITO-free perovskite solar cells without HTL based on the transparent polymer electrodes

Three transparent conductive electrodes (PH1000-5%, PH1000-10%, and PH1000-H) were made from PH1000 on glass substrates. The electrodes PH1000-5% and PH1000-10% were obtained from spin-coating the PH1000 solutions containing 5 vol% and 10 vol% DMSO on glass, respectively, at 3000 rpm for 40 s and dried at 140°C for 15 min. The PH1000 solutions were filtered through a 0.45 μm filter prior to being spin-coating on glass. The electrode PH1000-H was prepared as described below: PH1000 aqueous was first spin-coated onto the glass substrate at 3000 rpm for 40 s and dried in oven at 140°C for 15 min. DMSO solution of *p*-toluenesulfonic acid was then spin-coated on the formed PH1000 film at 3000 rpm for 40 s and dried at 140°C for 15 min again, followed by washingwith IPA three times to remove the residue acid and dried at 140°C.The fabricated three PH1000 electrodes on glass substrates were transferred into glovebox. Perovskite (0.8 M $PbCl_2$ and 2.4M CH_3NH_3I dissolved in DMF solution) was spin-coated on the electrode at 2000 rpm for 40s. After heating at 90°C for 2 hours, an electron transport layer of $PC_{61}BM$ (20 mg/ml, chlorobenzene solution) was spin-coated on the perovskite layer at 1500 rpm for 60s followed by spin-coating ZnO NPs solution at 4000 rpm for 35s. Finally, the substrates were transferred into a vacuum chamber to deposit 100 nm thick aluminum by thermal evaporation at a base pressure of 2×10^{-6} mbar. The completed devices (glass/PH1000/Perovskite/$PC_{61}BM$/ZnO/Al) were stored in N_2-purged glove box. The active device area was 4.2 mm^2.

2.2.2. ITO-free perovskite solar cells with HTL based on the transparent polymer electrodes

The perovskite solar cells with HTL were prepared with the same procedures as that for PSCs without HTL described above, with the exception that HTL of PEDOT:PSS was inserted between electrode PH1000 and perovskite. The PEDOT:PSS layer was spin-coated on electrodes at 3000 rpm followed by drying at 140°C for 15 min. To improve the wettability between electrode PH1000-H and PEDOT:PSS, 10 vol% IPA was added into PEDOT:PSS before spin-coating[36-38].

3. Results and discussion

3.1. Properties of transparent electrode PH1000

Transmittance and sheet resistance of electrodes (PH1000-5%, PH1000-10% and PH1000-H) at varies thickness are presented in Figure 1a. The thickness of the film was controlled by spinning speed. The transmittance and sheet resistance decreases as the thickness increases. For example, the transmittance increases from 85.3% to 88.5% when thickness decreases from 148 nm to 52 nm. The variation of optical transmittance of different PH1000 films is within 0.5% with the same thickness which can be regarded as measurement error. The sheet resistance of PH1000 films reduced by three orders after treated by different methods due to the phase separation between PEDOT and PSS and conformational change of PEDOT[39]. For example, when the film thickness is 68 nm, the sheet resistance of PH1000-10% is lower than PH1000-5% due to the higher concentration of DMSO can remove insulated PSS more effectively[34, 40]. It's worth noting that the sheet resistance of PH1000-H does not change much with different thicknesses, almost the same

around 143 Ω. This is attributed to the better ability to remove insulated PSS of *p*-toluenesulfonic acid than pure DMSO[34, 40].

Typical transmittance spectra of ITO and PH1000-10% electrodes are presented in Figure 1b. PH1000-10% film shows high transparency in the overall UV-visible range and even higher than ITO in the range from 300 nm to 570 nm, thus it's promising to replace ITO.

3.2. ITO and HTL free PSCs

Figure 2a shows the schematic architecture of PSCs built on ITO and PH1000 electrodes with or without HTL. The two typical cross-sectional SEM images of the completed devices are shown in Figures 2b and 2c. The thicknesses of perovskite layer in both devices are nearly the same, around 330 nm. The J-V and EQE curves of the PSCs are presented in Figure 3 and the photovoltaic parameters are summarized in Table 1.

As shown in Table 1, PSC based on ITO without HTL is shorted due to the large pinholes in the perovskite layer which will show later. The devices based on PH1000-5% and PH1000-10% without HTL however show much better performance than that built on bare ITO. The device based on PH1000-5% has a V_{OC} of 0.87 V, a J_{SC} of 15.65 mA/cm^2, a FF of 51.52%, and a PCE of 7.05%. The device based on PH1000-10% has nearly the same V_{OC} but higher J_{SC} and FF than the one based on PH1000-5%. This was mainly due to the higher conductivity of PH1000-10% which leads to lower series resistance (see Figure 1). The highest average PCE of 7.95% is obtained for the devices based on PH1000-10%. PH1000-H electrode has a smaller sheet resistance than PH1000-5% and PH1000-10% electrodes. However, it has a much poor efficiency of 1.22%. The J_{SC} calculated by integrating of the EQE spectra with the AM 1.5G solar flux is 16.63 mA/cm^2 for PSCs built on PH1000-10% which is corresponding to the J_{SC} calculated from I-V curve. The higher EQE of devices built on PH1000-10% and PH1000-H/ PEDOT:PSS-IPA in the range from 430 nm to 580 nm can be attributed to the higher transmittance of PH1000 films.

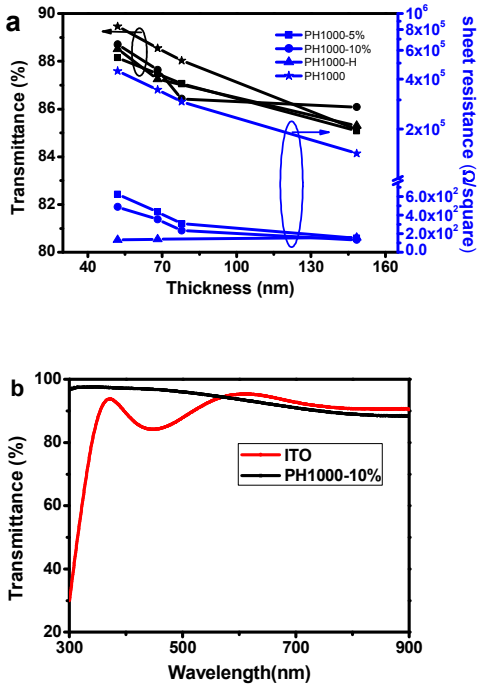

Figure 1. a) Transmittance spectra and sheet resistance of ITO and PH1000-10% (68 nm) films. b) Transmittance at 500 nm and sheet resistance of PH1000-5%, PH1000-10%, and PH1000-H films as a function of film thickness controlled by spin speed (spin speed of 1000, 2000, 3000, and 4000 rpm correspond to thickness of 148, 78, 68, and 52 nm).

It's well known that the morphology of the perovskite films significantly affects the performance of PSCs[41, 42]. Figure 4a, b, c, d shows the SEM images of perovskite films grown on ITO and PH1000-5%, PH1000-10% and PH1000-H electrodes without HTL respectively. We find that there are many large pinholes of perovskite film grown directly on ITO which lead to shorting of PSCs as indicated in Table 1. When PH1000-5% or PH1000-10% was used to replace ITO electrode, the surface coverage of perovskite was improved due to the similar surface property of PH1000 and PEDOT:PSS. It suggests PH1000-5% and PH1000-10% can be used to replace ITO to prepare device without HTL. However, there are some white regions in perovskite grown on PH1000-H (Figure 4d) . The white region B was characterized by EDX (see Table 2) which suggested it is PbI_2. The EDX in Table 2 shows significant increase of Pb and I compared to the ones in region A. Because EDX only determines the composition qualitatively, there is a difference between measured atom ratio and the theoretical atom ratio. N atom is believed to be contributed by $CH_3NH_3PbI_3$ and the increase of Pb atom ratio in region B compared to region A is believed to be resulted from the decomposition of $CH_3NH_3PbI_3$[43, 44]. It suggests the decomposition of perovskite can be accelerated by acidic substrate. So the device built on PH1000-H shows poor performance with a V_{OC} of 0.44 V, a J_{SC} of 9.99 mA/cm^2, a FF of 26.94%, and a PCE of 1.22%.

Figure 5 shows AFM images of PH1000-5%, PH1000-10% and PH1000-H conductive films. Figure 5b, 5d, 5f show their phase images. The conductive network can be seen clearly. The roughness of PH1000-5% calculated from Figure 5a is 0.89 nm. When the concentration of DMSO increases to 10% in PH1000 solution, the roughness of the formed film increases to 1.76 nm

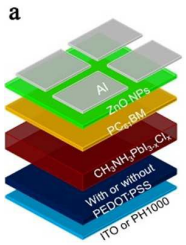

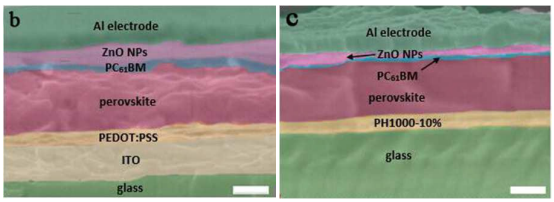

Figure 2. Cross-sectional SEM images showing the complete cell architecture. a) Schematic architecture of PSCs. The colored layer from bottom to up is b) glass, ITO, PEDOT:PSS, $CH_3NH_3PbI_{3-x}Cl_x$, $PC_{61}BM$, ZnO NPs, Al, c) glass, PH1000-10%, $CH_3NH_3PbI_{3-x}Cl_x$, $PC_{61}BM$, ZnO NPs, Al respectively. Both the bars are 200 nm.

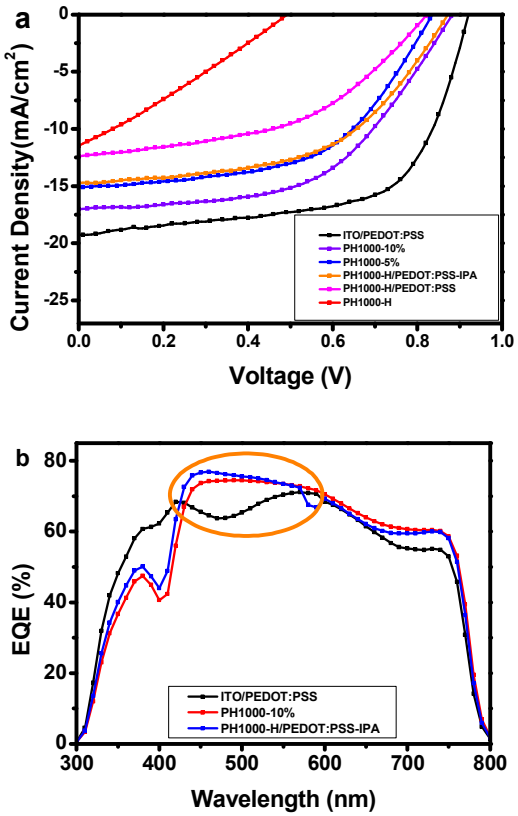

Figure 3. a) J-V curves of the devices based on different electrodes. The structure of device is electrode/$CH_3NH_3PbI_{3-x}Cl_x$/$PC_{61}BM$/ZnO NPs/Al. b) EQE characteristics of three type devices studied on this work. The integral current of the device based on ITO/PEDOT:PSS, PH1000-10%, PH1000-H/PEDOT:PSS-IPA is J_{SC1}=16.01 mA/cm^2, J_{SC2}=16.67 mA/cm^2, J_{SC3}=16.63 mA/cm^2 respectively.

(Figure 5c), almost twice of PH1000-5%. The roughness of PH1000-H film (Figure 5e) is 1.12 nm which is smoother than PH1000-10% but rougher than PH1000-5%. A rougher surface may be beneficial for hole exaction and lead to higher efficiency of solar cells[45, 46].The better device performance for PH1000-10% electrode based solar cell can be partly resulted from its rougher surface[45, 46].

Figure 6 shows the UPS of different films. It suggests that the ITO shows a work function of 4.5 eV while PH1000-5% shows a work function of 4.8 eV. When the concentration of DMSO increases to 10%, the work function of PH1000-10% decreases to 4.4 eV. The work function of PH1000-H further decreases to 4.2 eV due to higher ratio of PEDOT. However, the devices built on PH1000-5% and PH1000-10% show the same open-circuit voltage and the device built on PH1000-H shows a much lower V_{OC} of 0.44 eV which might be resulted from the poor surface coverage of perovskite. This suggests the surface coverage of perovskite has more significant effect on V_{OC}[47].

3.3. ITO-free PSCs with HTL

The devices built on ITO and PH1000 electrodes with HTL were fabricated. Their *J-V* curves and EQE spectra are presented in Figure 3 and the photovoltaic parameters are summarized in Table 1. Compared with the device built on ITO without HTL, the device built on ITO with PEDOT:PSS as HTL shows much better performance, with a V_{OC} of 0.91 V, a J_{SC} of 19.52 mA/cm^2, a FF of 62.45% and a PCE of 11.09%. Similarly as shown above, device built on PH1000-H shows much worse efficiency of 1.22% due to the decomposition of perovskite. Coating a layer of PEDOT:PSS on PH1000-H recovers the efficiency to 4.78% with a V_{OC} of 0.86 V. The higher series resistance of devices based on PH1000-H with HTL than device based on PH1000-5% and PH1000-10% is caused by the less conductive PEDOT:PSS which leads to lower efficiency of devices. After being treated by p-toluenesulfonic acid, part of hydrophilic PSS in PH1000 film was removed, leaving conductive hydrophobic PEDOT[34, 40]. Figure 7a shows the contact angle of PEDOT:PSS droplet on PH1000-H film. Hydrophobic surface of PH1000-H lead to a relatively large contact angle of 55.4°. Here 10% IPA was added into PEDOT:PSS aqueous to reduce the surface energy (Figure 7b) and the contact angle was reduced dramatically from 55.4° to 23.3°. So a thicker layer of PEDOT:PSS HTL can be obtained at the same spin coating rate (112 nm and 83 nm for PEDOT:PSS with or without IPA respectively which is measured by AFM).

Figure 4e, f, g shows the SEM images of perovskite grown on ITO/PEDOT:PSS, PH1000-H/PEDOT:PSS and PH1000-H/PEDOT:PSS -IPA respectively. Compared with the perovskite films grown on ITO and PH1000-H electrode, the surface coverage of the perovskite films is dramatically improved when growing on PEDOT:PSS HTL which coated on electrode.

Table 1. Photovoltaic performance based on different electrodes. The structure of solar cell is electrode/with or without HTL/$CH_3NH_3PbI_{3-x}Cl_x$/$PC_{61}BM$/ZnO NPs/Al

Electrode	HTL	V_{OC}(V)	J_{SC}(mA/cm^2)	FF(%)	PCE(%)	R_S(Ω)
ITO		0	0	0	0[a]	-

PH1000-H		0.44±0.10	9.99±1.44	26.94±2.47	1.22±0.27(2.27)	-
PH1000-5%		0.87±0.01	15.65±0.58	51.52±3.58	7.05±0.60(8.18)	2.0
PH1000-10%		0.88±0.03	16.88±1.09	53.44±3.28	7.95±0.57(9.65)	1.9
ITO	PEDOT:PSS	0.91±0.01[b]	19.52±0.85	62.45±0.80	11.09±0.67(12.03[c])	1.3
PH1000-H	PEDOT:PSS	0.86±0.04	12.12±1.51	46.37±6.03	4.78±0.65(6.11)	3.2
PH1001-H	PEDOT:PSS-IPA	0.89±0.02	14.83±0.67	52.58±4.25	6.98±0.66(9.31)	2.3

[a]*short circuit* [b]*standard deviation* [c]*highest efficiency*

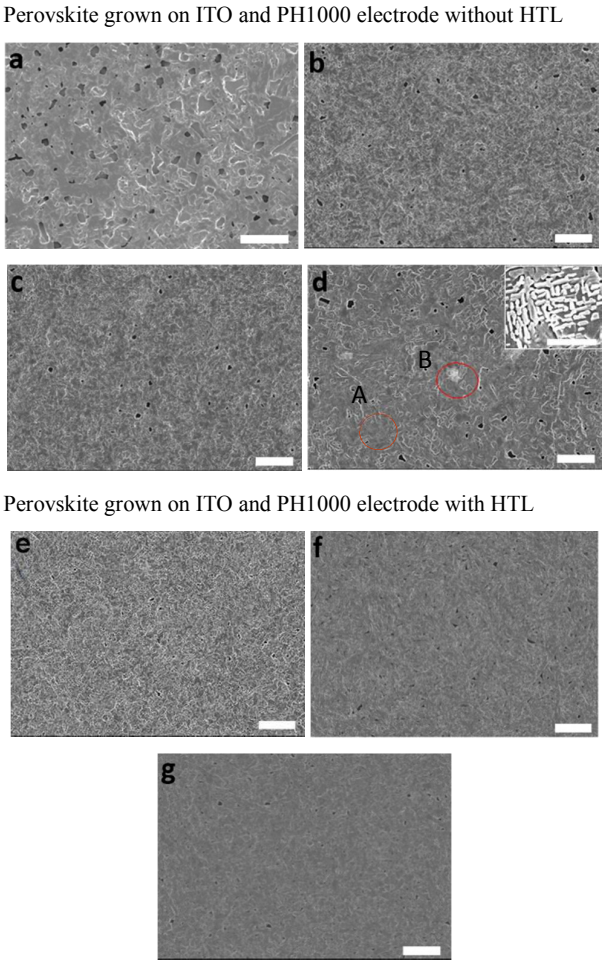

Figure 4. SEM images of perovskite $CH_3NH_3PbI_{3-x}Cl_x$ films on a) ITO, b) PH1000-5%, c) PH1000-10% , d) PH1000-H, e) ITO/PEDOT:PSS, f) PH1000-H/PEDOT:PSS. g) PH1000-H/PEDOT:PSS-IPA. The bar of a, b, c, d, e, f, g is 5 μm and the bar of image inside d is 500 nm.

grown on PH1000-H/PEDOT:PSS shows relatively more pin holes caused by the acidic PH1000-H. To protect perovskite from decomposing, a thicker and more uniform barrier layer of PEDOT:PSS is needed. 10% IPA was added into PEDOT:PSS to reduce surface energy and increase film thickness (from 83 nm and 112 nm). The surface coverage of perovskite grown on PH1000-H/PEDOT:PSS-IPA is higher than that grown on PH1000-H/PEDOT:PSS and is similar with that grown on ITO/PEDOT:PSS. The device built on PH1000-H/PEDOT:PSS-IPA shows better performance than device based on PH1000-H/PEDOT:PSS with an average PCE of 6.98%.

Figure 5a, 5c, 5e shows the morphology images of ITO/PEDOT:PSS, PH1000-H/PEDOT:PSS and PH1000-H/ PEDOT:PSS-IPA respectively. Coating a layer of PEDOT:PSS on PH1000-H reduces the roughness from 1.12 nm to 0.75 nm. Adding 10% IPA into PEDOT:PSS shows a similar roughness of 0.87 nm and nearly the same with the roughness of PEDOT:PSS on ITO of 0.66 nm.

From the UPS results shown in Figure 6, we find that, no matter what the electrode is, the work function recovers to 5.0 eV when coating a layer of PEDOT:PSS. Coating a layer of PEDOT:PSS on PH1000-H not only protects perovskite from decomposing, but also reduces the energy barrier between electrode and perovskite significantly. 10% IPA that added into PEDOT:PSS can further increase the work function of PH1000-H/PEDOT:PSS-IPA slightly by about 0.1 eV to 5.1 eV. It's beneficial for hole extraction and thus a better PSCs performance. Due to the similar work function when

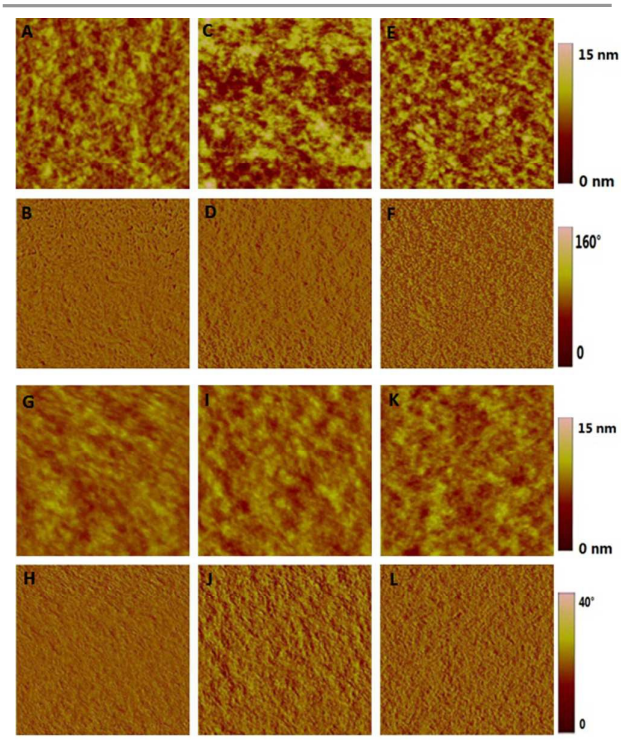

Figure 5. a, c, e, g, i, k are the morphology images of PH1000-5%, PH1000-10%, PH1000-H, ITO/PEDOT:PSS, PH1000-H/PEDOT:PSS and PH1000-H/PEDOT:PSS-IPA films, respectively. And b, d, f, h, j, l are the corresponding phase images. The roughness of a, c, e, g, i, k is 0.89, 1.76, 1.12, 0.66, 0.75 and 0.87 nm, respectively. The size of images is 1.5 μm×1.5 μm.

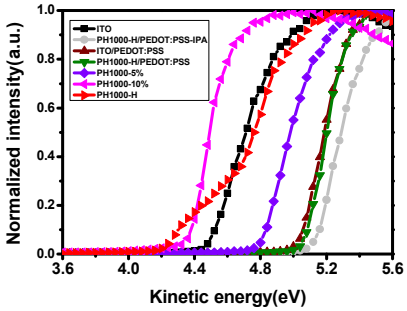

Figure 6. UPS of ITO, ITO/PEDOT:PSS, PH1000-H/PEDOT:PSS, PH1000-H/PEDOT:PSS - IPA, PH1000-5%, PH1000-10%, and PH1000-H films. The work function is 4.5 eV, 5.0 eV, 5.0 eV, 5.1 eV, 4.8 eV, 4.4 eV, 4.2 eV respectively.

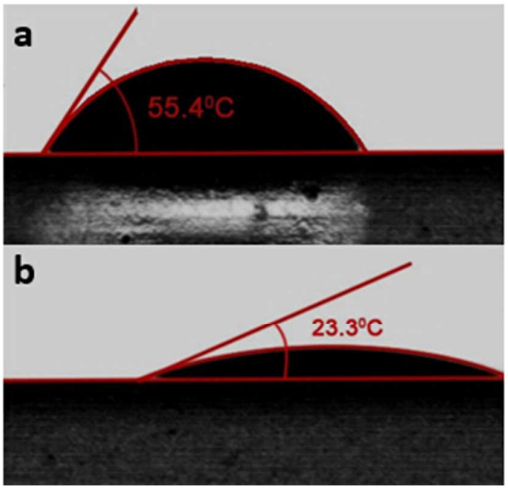

Figure 7. Contact angle of a) 10 µl PEDOT:PSS droplet and b) 10 µl PEDOT:PSS droplet containing 10% IPA on glass/PH1000-H films. These images were taken by water contact angle equipment and the angle was calculated automatically.

Table 2. A) the composition in region A in Figure 4d, B) the composition in region B in Figure 4d, characterized by EDX.

	Element	*Wt%*	*At%*
A	N	5.38%	19.53%
	Pb	27.01%	6.62%
	I	53.05%	21.25%
B	N	2.65%	14.00%
	Pb	37.84%	13.53%
	I	51.43%	30.03%

coating a layer of PEDOT:PSS on electrodes and the similar surface coverage of perovskite film, the devices built on PH1000 electrode with HTL show similar open-circuit voltage. Device based on PH1000-H/PEDOT:PSS-IPA shows better performance with a V_{OC} of 0.89 V, a J_{SC} of 14.83 mA/cm^2, a FF of 52.58% and a PCE of 6.98%. The J_{SC} calculated by integrating of the EQE spectra with the AM 1.5G solar flux is 16.63 mA/cm^2 and 16.01 mA/cm^2 for PSCs built on PH1000-H/PEDOT:PSS-IPA and ITO/PEDOT:PSS respectively which is corresponding to the J_{SC} calculated from *I-V* curve.

4. Conclusions

In summary, we successfully employ low temperature processed conductive polymer PH1000 material as an alternative electrode material of ITO to fabricate HTL-free PSCs. The optimized average PCE of 7.95% with the highest PCE up to 9.65% for PSCs built on PH1000-10% electrode without HTL was achieved. When a layer of PEDOT:PSS was spin coated on PH1000-H to prevent perovskite from decomposing, the optimized PCE of 6.98% with the highest up to 9.31% was achieved. Our results indicate that PH-1000 is a promising material to replace both ITO electrode and HTL, providing a much simpler architecture for flexible PSC applications.

Acknowledgements

This work was supported by the Major State Basic Research Development Program (2014CB643503), the National Natural Science Foundation of China (Grants 91233114, 51261130582), and the Fundamental Research Funds for the Central Universities (Grant No. 2015FZA4008).

References

1. W. S. Yang, J. H. Noh, N. J. Jeon, Y. C. Kim, S. Ryu, J. Seo and S. I. Seok, *Science*, 2015.
2. M. M. Lee, J. Teuscher, T. Miyasaka, T. N. Murakami and H. J. Snaith, *Science*, 2012, 338, 643-647.
3. J. M. Ball, M. M. Lee, A. Hey and H. J. Snaith, *Energ Environ Sci*, 2013, 6, 1739-1743.
4. L. Zuo, Z. Gu, T. Ye, W. Fu, G. Wu, H. Li and H. Chen, *J Am Chem Soc*, 2015, 137, 2674-2679.
5. L. Wang, W. Fu, Z. Gu, C. Fan, X. Yang, H. Li and H. Chen, *J Mater Chem C*, 2014, 2, 9087-9090.
6. Z. Gu, F. Chen, X. Zhang, Y. Liu, C. Fan, G. Wu, H. Li and H. Chen, *Sol Energ Mat Sol C*, 2015, 140, 396-404.
7. J. Muller, B. Rech, J. Springer and M. Vanecek, *Sol Energy*, 2004, 77, 917-930.
8. K. Ellmer, *Nat Photonics*, 2012, 6, 808-816.
9. R. Tahar, T. Ban, Y. Ohya and Y. Takahashi, *J Appl Phys*, 1998, 83, 2631-2645.
10. S. RAY, R. BANERJEE, N. BASU, A. K. BATABYAL and A. K. BARUA, *J Appl Phys*, 1983, 54, 3497-3501.
11. A. E. Rakhshani, Y. Makdisi and H. A. Ramazaniyan, *J Appl Phys*, 1998, 83, 1049-1057.
12. B. Augustine, R. Sliz, K. Lahtonen, M. Valden, R. Myllylä and T. Fabritius, *Sol Energ Mat Sol C*, 2014, 128, 330-334.
13. M. Dianetti, F. Di Giacomo, G. Polino, C. Ciceroni, A. Liscio, A. D'Epifanio, S. Licoccia, T. M. Brown, A. Di Carlo and F. Brunetti, *Sol Energ Mat Sol C*, 2015, 140, 150-157.
14. K. Sun, P. Li, Y. Xia, J. Chang and J. Ouyang, *Acs Appl Mater Inter*, 2015, 7, 15314-15320.
15. M. Layani, A. Kamyshny and S. Magdassi, *Nanoscale*, 2014, 6, 5581-5591.
16. W. Cao, J. Li, H. Chen and J. Xue, *J Photon Energy*, 2014, 4.
17. R. K. de Castro, J. R. Araujo, R. Valaski, L. O. O. Costa, B. S. Archanjo, B. Fragneaud, M. Cremona and C. A. Achete, *Chem Eng J*, 2015, 273, 509-518.
18. K. Lai, C. Liu, C. Lu, C. Yeh and M. Houng, *Sol Energ Mat Sol C*, 2010, 94, 397-401.
19. Q. Yan, Z. Gu, Q. Li, W. Fu, X. Chen, W. Liu, H. Pan, M. Wang and H. Chen, *Chinese J Polym Sci*, 2014, 32, 395-401.
20. J. Han, S. Yuan, L. Liu, X. Qiu, H. Gong, X. Yang, C. Li, Y. Hao and B. Cao, *J Mater Chem A*, 2015, 3, 5375-5384.
21. K. Poorkazem, D. Liu and T. L. Kelly, *J Mater Chem A*, 2015, 3, 9241-9248.

22. J. Fan, B. Jia and M. Gu, *Photonics Research*, 2015, 2, 111-120.
23. L. Hu, H. S. Kim, J. Lee, P. Peumans and Y. Cui, *Acs Nano*, 2010, 4, 2955-2963.
24. S. De, T. M. Higgins, P. E. Lyons, E. M. Doherty, P. N. Nirmalraj, W. J. Blau, J. J. Boland and J. N. Coleman, *Acs Nano*, 2009, 3, 1767-1774.
25. M. Lee, Y. Jo, D. S. Kim and Y. Jun, *J Mater Chem A*, 2015, 3, 4129-4133.
26. J. Troughton, D. Bryant, K. Wojciechowski, M. J. Carnie, H. Snaith, D. A. Worsley and T. M. Watson, *J Mater Chem A*, 2015, 3, 9141-9145.
27. F. Jiang, T. Liu, S. Zeng, Q. Zhao, X. Min, Z. Li, J. Tong, W. Meng, S. Xiong and Y. Zhou, *Opt Express*, 2015, 23, A83-A91.
28. F. Jiang, T. Liu, S. Zeng, Q. Zhao, X. Min, Z. Li, J. Tong, W. Meng, S. Xiong and Y. Zhou, *Opt Express*, 2015, 23, A83-A91.
29. J. Lee, J. Seong, J. Park, S. Park, D. Lee and K. Shin, *Mech Syst Signal P*R, 2015, 60-61, 706-714.
30. Y. Deng, P. Yi, L. Peng, X. Lai and Z. Lin, *J Micromech Microeng*, 2015, 25.
31. Y. Jin and G. Chumanov, *Acs Appl Mater Inter*, 2015, 7, 12015-12021.
32. P. Bhatt, K. Pandey, P. Yadav, B. Tripathi, C. K. P., M. K. Pandey and M. Kumar, *Sol Energ Mat Sol C*, 2015, 140, 320-327.
33. Y. H. Kim, C. Sachse, M. L. Machala, C. May, L. Mueller-Meskamp and K. Leo, *Adv Funct Mater*, 2011, 21, 1076-1081.
34. Y. Hsiao, W. Whang, C. Chen and Y. Chen, *Journal Of Materials Chemistry*, 2008, 18, 5948-5955.
35. L. Qian, J. Yang, R. Zhou, A. Tang, Y. Zheng, T. Tseng, B. Debasis, J. Xue and P. H. Holloway, *Journal Of Materials Chemistry*, 2011, 21, 3814.
36. E. Y. Choi, J. H. Seo, H. M. Kim, J. H. Kim, J. T. Je and Y. K. Kim, *Inec: 2010 3rd International Nanoelectronics Conference*, VOLS 1 AND 2, 2010, 921-922.
37. W. Zhang, X. Bi, X. Zhao, Z. Zhao, J. Zhu, S. Dai, Y. Lu and S. Yang, *Org Electron*, 2014, 15, 3445-3451.
38. E. Y. Choi, J. H. Seo, H. M. Kim, J. H. Kim, J. Je and Y. K. Kim, *Inec: 2010 3rd International Nanoelectronics Conference*, VOLS 1 AND 2, 2010, 921-922.
39. J. Ouyang, *Acs Appl Mater Inter*, 2013, 5, 13082-13088.
40. S. Mukherjee, R. Singh, S. Gopinathan, S. Murugan, S. Gawali, B. Saha, J. Biswas, S. Lodha and A. Kumar, *Acs Appl Mater Inter*, 2014, 6, 17792-17803.
41. G. E. Eperon, V. M. Burlakov, P. Docampo, A. Goriely and H. J. Snaith, *Adv Funct Mater*, 2014, 24, 151-157.
42. P. Liang, C. Liao, C. Chueh, F. Zuo, S. T. Williams, X. Xin, J. Lin and A. K. Y. Jen, *Adv Mater*, 2014, 26, 3748-3754.
43. K. Sun, P. Li, Y. Xia, J. Chang and J. Ouyang, *Acs Appl Mater Inter*, 2015, 7, 15314-15320.
44. J. Yang, B. D. Siempelkamp, E. Mosconi, F. De Angelis and T. L. Kelly, *Chem Mater*, 2015, 27, 4229-4236.
45. J. R. Jennings, A. Ghicov, L. M. Peter, P. Schmuki and A. B. Walker, *J Am Chem Soc*, 2008, 130, 13364-13372.
46. N. Tetreault, E. Horvath, T. Moehl, J. Brillet, R. Smajda, S. Bungener, N. Cai, P. Wang, S. M. Zakeeruddin, L. Forro, A. Magrez and M. Graetzel, *Acs Nano*, 2010, 4, 7644-7650.
47. Z. Liu and E. Lee, *Org Electron*, 2015, 24, 101-105.